AIRBORNE RADAR SOUNDING OF THE GREENLAND ICE SHEET[1]

EDMUND F. PAWLOWICZ

Department of Geology, Bowling Green State University, Bowling Green, Ohio 43403

ABSTRACT

Radar sounding is a technique used in recent years to determine the thickness of ice sheets and glaciers. A radar signal is transmitted through ice, a dielectric, is reflected from the bottom, and is received at some time after its transmission. The length of time which the radar pulse spends in the ice, the so-called "delay time of the pulse," can be related empirically to the thickness of ice sheets and glaciers with a maximum uncertainty of approximately 2 percent without considering errors in positioning, electronics, and other conditions.

Airborne radar sounding was used, in 1966, to sound successfully nearly 10,000 km of the Greenland ice sheet, penetrating the ice to a depth of up to 3,000 m. This method is rapid, mobile, and accurate when compared with more conventional techniques and should prove to be a most valuable tool for the study of the thickness of glacial ice.

INTRODUCTION

A recently developed electromagnetic technique known as radar sounding has been used successfully to collect data permitting the calculation of the thickness of ice sheets and glaciers. This method has been used to obtain such measurements at stations located both on the ice surface (Jiracek, 1965; Weber and Andrieux, 1970) and airborne, in operations over the Greenland and Antarctic ice sheets (Swithenbank, 1967). The more recent work in Greenland by myself and others (Walker, Pearce, and Zanella, 1968; Pawlowicz, 1969) involved a more precise application of this technique, with the use of mathematical relationships which incorporate variations of the dielectric properties of ice with depth.

In July, 1966, the U. S. Army Electronics Command Arctic and Antarctic Research Team, of which the author was a member, flew in an EC-121-P (Super Constellation) over the Greenland Ice Sheet and collected what was probably ice-thickness data on this ice sheet than all of the previous national and international expeditions combined (C. B. B. Bull, personal communication, 1969). Ice thicknesses of nearly 3000 m were sounded successfully. The empirical method which was used to reduce the ice-thickness data and a summary of some of the ice-thickness results obtained in this survey are presented in this paper.

The data reported here were obtained from flights originating at Thule Air Force Base and at Søndre Strømfjord Air Force Base in Greenland. Supplemental weather data used in computing navigational fixes came from Camp Century (located at 77° 10′ 22″ N, 61° 08′ 42″ W) and from Blue Ice (located at 77° 56′ 48″ N, 39° 11′ 00″ W).

THEORY

Ice, being a dielectric, can propagate electromagnetic waves. In the airborne determination of ice thickness, a radar pulse is transmitted, which is propagated through air at the free-space velocity, c, (300 m μsec $^{-1}$) and then intersects the air-ice interface (figs. 1 and 2). Fresnel's and Snell's equations (see, for example, Von Hipple, 1954) for the reflection and transmission of electromagnetic energy may be applied; the signal propagated into the ice is reduced by 10 log $(1-|R_1|^2)$ db, where R_1 is the reflection coefficient of the air-ice boundary (and db is the abbreviation for decibels).

The radar pulse then travels through the ice, is reflected from the ice-subice interface, losing 10 log$|R_2|$db, where R_2 is the reflection coefficient of the ice-

[1]Manuscript received October 13, 1971.

subice contact, and returns through the ice and air to the aircraft. The returning signal is reduced by an additional 10 log $(1-|R_1|^2)$ db at the ice-air contact.

The pulse reflected from the bottom of the ice, B, is delayed in time relative to the pulse reflected from the surface, S, by $2\Delta t$, twice the one-way travel time of the pulse in ice. This travel time, Δt, may be used to calculate the corresponding ice thickness, H, if the relationship between the two parameters is known.

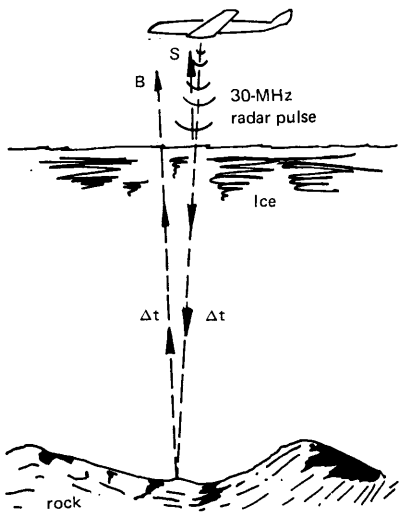

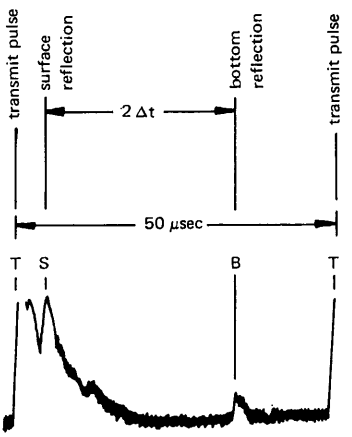

FIGURE 1 (left). Ray paths of the radar signals. In this figure, S is the pulse reflected from the ice surface, and B is the pulse reflected from the bottom of the ice (from Walker, Pearce, and Zanella, 1968).

FIGURE 2 (right). Oscilloscope display of typical radar pulses. In this figure, T is the transmitted pulse, S is the pulse reflected from the ice surface, and B is the pulse reflected from the bottom of the ice (from Walker, Pearce, and Zanella, 1968).

EMPIRICAL RELATIONSHIPS

Investigators have used many approaches to obtain empirical equations relating the electromagnetic propagation velocity or, equivalently, the relative dielectric constant to ice depth. One method, discussed by Jiracek (1965), is similar to that used for calculating the variation of seismic-wave velocity with depth, and involves determining the variation of reflection time from a given point on the interface. A plot of the square of the reflection time, t^2, versus the square of the horizontal distance from the sound source, x^2, gives the average acoustic velocity of propagation at the location.

An alternative approach, which is presented in this paper, utilizes an empirical equation relating the variation of the relative index of refraction with ice depth. Note that, if the magnetization of a dielectric is neglected, the relative index of refraction, η, is related to the relative dielectric constant, k', in the following manner:

$$\eta = \sqrt{k'} \tag{1}$$

The optical-path length in a dielectric, such as ice, is defined as

$$L = c\Delta t, \tag{2}$$

where L = optical-path length (m),
c = speed of light (300 m μsec^{-1}), and
Δt = one-way travel time in ice (μsec).

Since $$\eta(x) = c/v(x), \tag{3}$$

where $\eta(x)$ = variation of relative index of refraction with ice depth, x, and
$v(x)$ = variation of electromagnetic wave velocity with ice depth, x,

equation (3) may be expressed as

$$c\Delta t = \int_0^H \eta(x)\, dx, \tag{4}$$

where H = ice thickness (m), and
x = vertical distance (m).

At Camp Century, Greenland, the variation of the relative index of refraction of ice with depth at a frequency of 30 MHz (Pearce and Walker, 1967) approximates a function of the form

$$\eta(x) = \frac{\eta_\infty x/a + \eta_o}{x/a + 1}, \tag{5}$$

where η_o = relative index of refraction just beneath the ice surface $(x \to 0)$,
η_∞ = relative index of refraction at great depth $(x \to \infty)$, and
a = best-fit scale factor (m).

For a near-surface snow density, ζ_o, equal to 0.34 g cm^{-3}, the corresponding relative index of refraction at 30 MHz, η_o, is 1.29 (Evans, 1965; Robin and Evans, 1967). The relative dielectric constant at the surface, k'_o, is 1.67. Using a least-squares error technique, the best fit of equation (5) to the Camp Century data on relative index of refraction yields a value of 10.2 m for the scale factor, a. Additionally, analysis of the same data suggests a value for the deep-ice relative dielectric constant, k'_∞, of 3.352.

Substituting equation (5) into equation (4) yields

$$c\Delta t = \int_0^H \left[\frac{\eta_\infty x/a + \eta_o}{x/a + 1} \right] dx, \tag{6}$$

which after integration gives

$$c\Delta t = \eta_\infty H - a(\eta_\infty - \eta_o) \ln\left(\frac{H+a}{a}\right). \tag{7}$$

The values of c, η_o, η_∞, and a at 30 MHz are known from the Camp Century data, so that given a value of the one-way travel time in ice, Δt, the corresponding ice thickness, H, can be calculated.

MEASUREMENT PROCEDURE

In July, 1966, ice-thickness data over a large portion of the ice sheet were obtained by U. S. Army Electronics team, which included the author, using a 30 MHz radar ice-sounding system, in a series of four flights over Greenland (fig. 3). Flights 1, 2, and 3 were flown from Thule Air Force Base, and Flight 4 from Søndre

Strømfjord Air Force Base. The four traverses averaged about eight hours of flight time, the total extent of ground covered being 9,600 km.

The EC–121–P (Super Constellation) airplane flew at an airspeed of approximately 320 km hr^{-1} at an altitude of 600 m above the surface of the ice. This altitude was selected to allow a clear separation between the transmitted pulse and the surface reflection, so that the total time in ice could be measured, and to provide adequate maneuvering space for the aircraft. Flying too high is disadvantageous, for not only are the transmission losses increased, but the pulse reflected from the bottom of the ice may interact with the next transmitted pulse. For example, given a pulse-repetition frequency of 20 kHz and an ice thickness of 3,000 m, the bottom reflection would be completely merged with the next transmitted pulse at an aircraft height of 2,100 m above the ice.

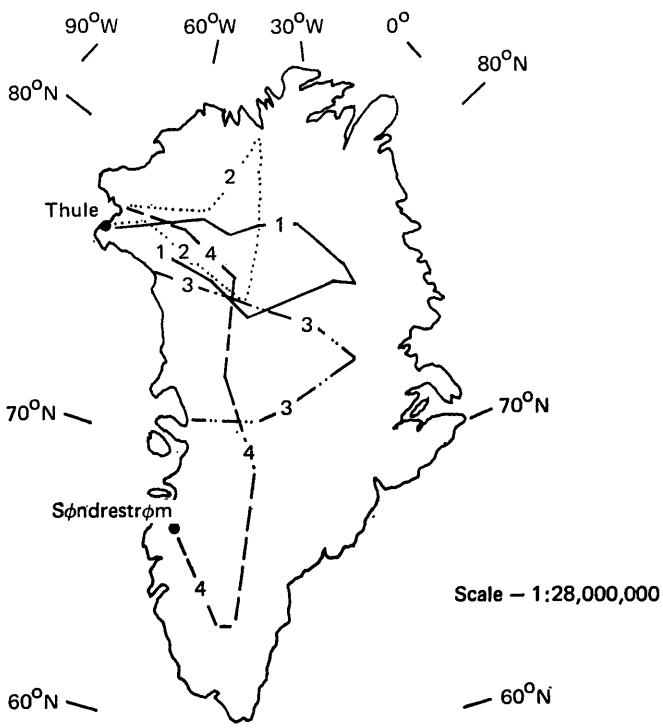

FIGURE 3. Map of Greenland showing the location of the 1966 airborne radar sounding traverses (from Walker, Pearce, and Zanella, 1968).

In order to plot ice-air and ice-subice surfaces as elevations above sea level, the height of the aircraft both above sea level and above the ice surface must be known. Thus, readings from the aircraft barometric altimeter and from the heading and airspeed indicators, located on the control operator's panel, were continuously observed and recorded. The barometric altimeter, reset at each takeoff and landing location, served as a guide to aircraft altitude; barometric pressures, corrected for temperature and humidity, all of which were recorded by the aerograph unit, were later converted to exact elevations above sea level by the barometric equation in conjunction with synoptic pressure charts. A strip-chart recorder continuously plotted the output of a 4,300 MHz radar altimeter, giving the aircraft height above the ice. This instrument, after being zeroed to

an altitude of 610 m, could track a change in height of ±150 m with a reading accuracy of ±3 m. At a few points, a comparison of the computed ice-surface elevations with the known elevations of surface reference points was possible.

To permit processing of the data, the three main recordings used in the ice-depth measuring system—for ice-thickness data, altitude information, and for navigation fixes—were synchronized in time, using the radio signal from CHU, Canada. Every five seconds, or about every ½ km of traverse, the calibrated timing circuit actuated the pulse-recording camera which photographed the ice-thickness output display. Each photographic frame had its associated time, flight, and frame number inscribed on it.

Position information during the flights, essential for interpreting these data, was accumulated by the late 1/LT Edward Taylor, USAF. Solar navigation was used for all locations except for those along a portion of Fight 4, over southern Greenland, where Loran fixes were possible. The positions indicated in Figure 3 represent fixes calculated primarily from solar navigation procedures. Constant airspeed and heading were usually maintained between the fixes, but occasionally, when the dorsal radome of the aircraft partially obscured the sun, course changes were made to permit a sextant sun shot.

The radar ice-thickness measurements, altimetry, and navigation were coordinated during the flights by a control operator, who maintained a log of all pertinent information, such as airspeed, heading and heading changes, barometric altimeter readings, and landmarks. The accumulation of ice-thickness data, however, was entirely automated, except for the periodic replenishment of recording film.

QUALITATIVE DESCRIPTION OF THE ICE-THICKNESS DISPLAYS

Examples of the airborne ice-thickness oscilloscope records (displays) with comparatively good reflections from the bottom of the ice sheet are given in Figures 4 and 5. The sharp bottom reflections suggest that the contact between the ice

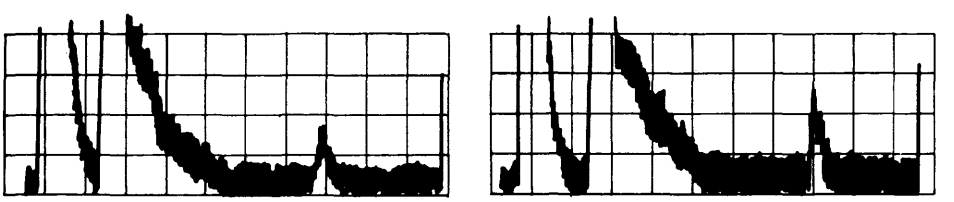

FIGURES 4–5. Oscilloscope output displays (H = 2,200 m).

and sub-glacial material, in these places, is very distinct and smooth within the beam width of the transmitted wave.

Although a good bottom reflection was usually recorded, occasionally the amplitude and width of the bottom pulse fluctuated irregularly over short distances, suggesting that the ice-subice contact was a little more irregular than the smooth bottom which generated the sharp pulse. In places, the bottom reflection changed from a completely readable pulse to one which was lost in the noise within the time period of adjoining frames. These changes in the quality of the bottom reflection are a measure of the smoothness, or the degree of specularity (relative to 5.6 m, the 30 MHz wavelength in ice) of the ice-subice contact in the area scanned by the finite beam width of the transmitted wave. To suggest a specific cause for the odd-shaped, pulsating bottom reflections would be presumptuous, since so little is known of the nature of the ice-subice contact. An example of a change in the quality of the bottom reflection in adjoining frames (5 sec) is given in Figures 6 and 7.

The bottom signal in some places was completely lost, a stituation that could be caused by absorption of the signal and other losses in extremely thick ice, or by unusually high reflection and absorption losses when the upper surface is realtively warm. In the majority of cases, loss of the bottom reflection was accompanied by an abnormally strong air-ice surface reflection, by relatively warm surface temperatures (−1°C at one station) and, occasionally, by meltwater pools on the ice surface, suggesting that the incident energy was largely reflected from the upper surface. Such lack of penetration was the primary reason that no ice-thickness data were obtained during the southerly leg of Flight 4.

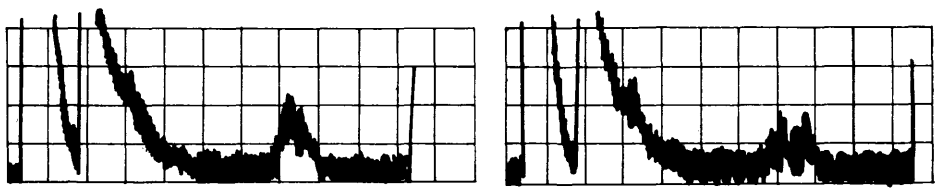

FIGURES 6–7. Oscilloscope output displays (H=2,150 m, t=22:34:40 Z−22:34:45 Z).

When the subglacial topography is mountainous, reflections from the sides of these mountains may be received along with those from the bottoms of the mountains, causing the signals received to be erratic and commonly obliterating the bottom reflection. A high-amplitude pulse can sometimes be discerned in the noise, but this pulse may be either a bottom reflection or the result of the addition of a number of waves received from points located at equal distance from, but not located directly beneath, the aircraft. Occasionally, a pulse which may be the bottom reflection can be correlated from data frame to data frame, but accepting this reflection as the pulse from the bottom is largely a matter of faith. Examples of oscilloscope displays when the subglacial topography is mountainous are given in Figures 8 and 9. For comparison, a display when the aircraft is flown over an exposed mountainous region is also shown (fig. 10).

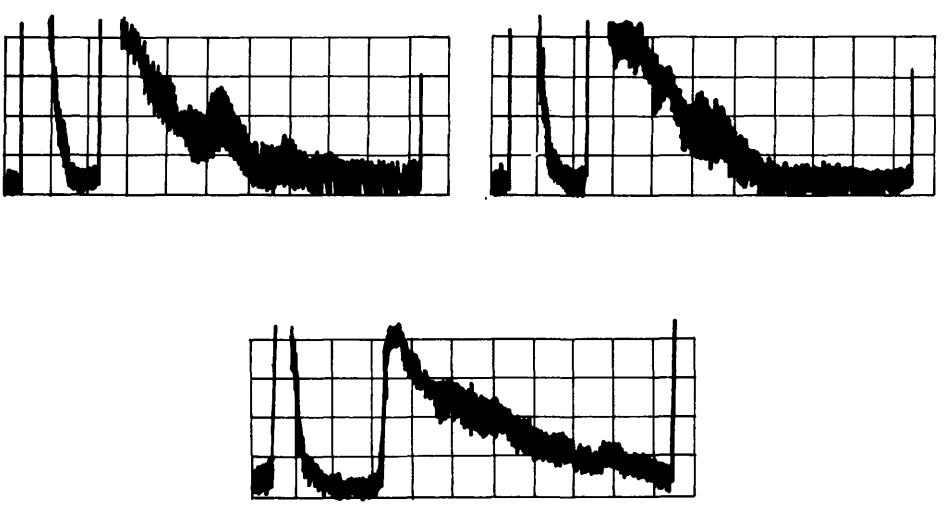

FIGURES 8–9 (top). Oscilloscope output displays over mountainous subglacial topography.
FIGURE 10 (bottom). Oscilloscope output display over exposed mountains (north of Søndre Strømfjord).

Reflections from intermediate layers in the ice, similar to those described by Bailey, Evans, and Robin (1964), by Jiracek (1965), and by Robin (1967), were observed in numerous locations in Greenland. An example of possible reflection from deep layers in the ice is given, in time sequence, in Figures 11 through 14.

Near-surface internal reflections commonly seen on the tail of the surface reflection are probably due to the annual layering in the firn and ice in the upper 50 to 100 m of the ice sheet. Extraneous reflections at greater depth are presumably from the surfaces of isolated "layers" within the ice, but whether these reflective layers are density contacts, stress variations, moraine brought up from the bottom along shear planes, or, possibly, volcanic ash, is uncertain.

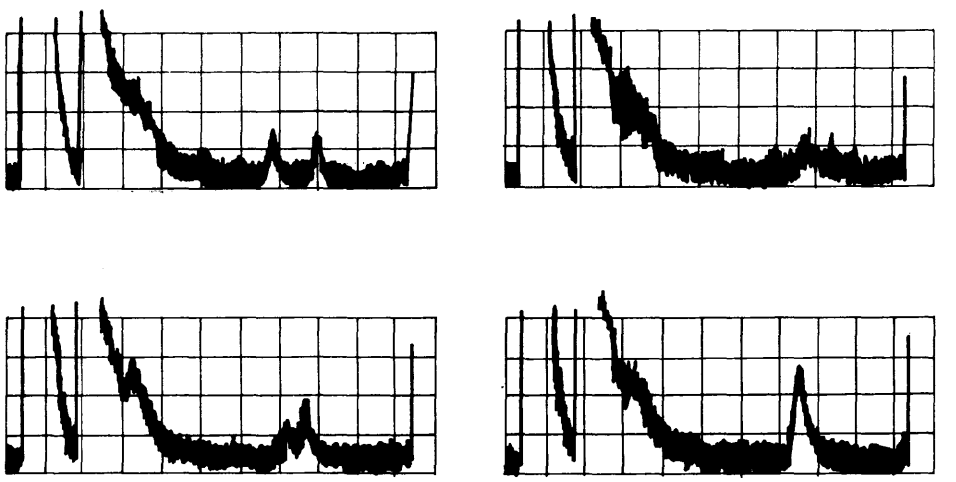

FIGURES 11–14. Oscilloscope output displays (t=22:34:05 Z−22:34:20 Z).

Additional data on deep-ice layers from an analysis of deep cores such as those obtained at Camp Century, Greenland, and at Byrd Station, Antarctica, are needed to identify the parameters which cause these intermediate echoes. The Byrd Station core (Gow, Ueda, and Garfield, 1968) consisted of a brecciated zone of ice, two layers of volcanic ash and a sharp change from bubbly to clear ice at about 1,300 m. Because the 30 MHz wavelength in ice is much greater than the thickness of the ash layers, these layers could theoretically cause intermediate reflections. Additional work correlating the depth of these internal reflections derived from radar measurements with the location of the inhomogeneities in the core needs to be performed in order to define more accurately the parameters which govern these reflections.

The qualitative description of the 30 MHz radar display is applicable to the data from all four flights. At present, however, only the data from Flight 1—ice-thickness values, altitudes, and navigation fixes—have been reduced, integrated, and analyzed; therefore it is only the results of this flight that are discussed in detail in this paper. Some of the ice-thickness values and navigation fixes for Flight 3 have been calculated, but results are not adequate for such a detailed discussion of these data. In both Flights 1 and 3, the overall quality of the bottom reflection was good, allowing excellent data recovery. The pulse reflected from the upper ice surface was 60 to 90 db above the receiver noise, while the bottom echo varied from the noise level to about 55 db above it.

DATA REDUCTION PROCEDURES

If the in-ice radar propagation time, Δt, is known, the corresponding ice thickness, H, can be calculated, using Equation 7. To eliminate computational error

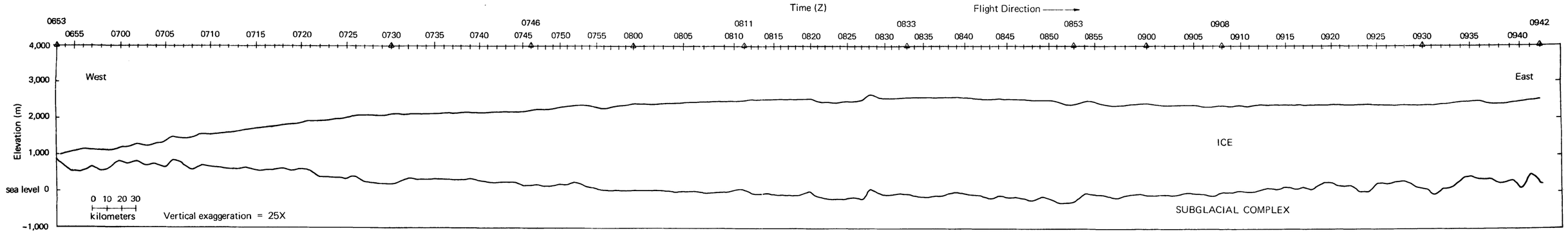

Eastbound Leg – Flight 1

Figure 16. Ice-thickness profile for eastbound leg of flight 1.

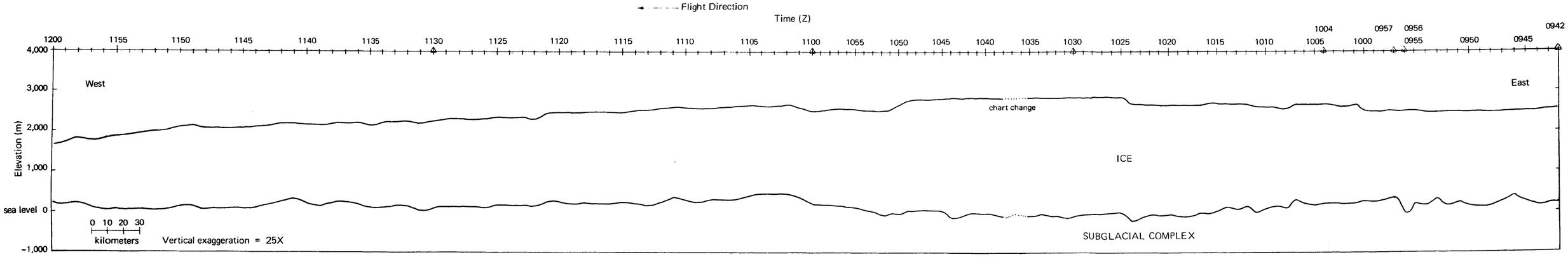

Westbound Leg – Flight 1

Figure 17. Ice-thickness profile for westbound leg of flight 1.

and to save time, the author used a digital computer to print out a table of delay times and ice thicknesses. The 35mm film from the data camera was read with a 20x viewer, which was equipped with movable, precision x and y crosshairs, calibrated in machine units. The time delays were measured from every data frame (every 5 seconds, or ½ km) for Flight 1. However, such detailed analyses were apparently not necessary, for a sampling of the data every 30 seconds where the ice-thickness change with distance was small, or every 15 seconds where the change was large would have been satisfactory for a general analysis of the subglacial topography. The time delays were then converted to ice thickness, using the computer print-out.

The elevation of the ice surface above sea level was calculated by subtracting the aircraft height above the ice surface—data recorded by the 4,300 MHz radar altimeter and recorder—from the aircraft elevation above sea level, which was computed from barometric pressure, temperature, and relative humidity data, using the barometric equation in conjunction with synoptic pressure charts. The navigation fixes were determined through use of solar navigation principles incorporating airspeed (about 320 km hr $^{-1}$), wind velocity, and supplemental weather data from Camp Century and Blue Ice.

ACCURACY OF THE DATA

The accuracy of the ice-thickness calculations for any given location is limited primarily by the uncertainty about the deep-ice relative index of refraction, η_∞, which is a function of ice density, temperature, and possibly stress and other variables. In the reduction of the airborne ice-thickness data, the variation of the relative index of refraction with depth measured at Camp Century (Pearce and Walker, 1967) is assumed to be applicable to the entire ice sheet, an assumption which necessarily causes an uncertainty in the thickness values.

The uncertainty in η_∞, neglecting temperature influences, contributes a possible error of 1.2 percent (Walker, Pearce, and Zanella, 1968); the uncertainty due to hypothetical temperature variations may be 0.7 percent where the average deep-ice temperatures are sufficiently different (as much as 20°C) from those at Camp Century. System errors—timing, pulse shaping, etc.—and data-reduction techniques contribute an additional uncertainty of 0.8 percent. The total uncertainty in the ice-thickness values is, therefore, about 2.0 percent, neglecting the temperature effects, and may be as much as 2.7 percent if these effects are considered.

To determine the accuracy of the elevation data for the ice surface, the calculated elevation must be compared with a known surface elevation. Because of navigation uncertainties, the number of such known surface elevation points is limited, but the few comparisons which could be made indicate that the computed elevations of the ice surface were within 50 m of the known surface elevation.

The assessment of the accuracy of the navigation data is likewise limited by the paucity of surface control points. Given this uncertainty, the error in the final course for Flight 1 (fig. 15) is considered to be within 4 km except for positions K, L, and M, which are thought to be within 16 km. In addition, some navigational errors were caused by a partial blocking of the sun by the dorsal radome of the aircraft when the sun shots were taken.

A BRIEF DISCUSSION OF THE ICE-THICKNESS VALUES OBTAINED FROM FLIGHT 1

Although four different flights were made, only the data from Flight 1 are complete enough and adequately analyzed to be presented here. The route of Flight 1 is shown in Figure 15, and the ice-thickenss profiles determined from these data are given in Figures 16 and 17. Some general comments about these profiles are presented below; however, for a more comprehensive discussion, the reader is referred to the paper by Walker, Pearce, and Zanella (1968).

At the extreme western end of the eastbound traverse, between stations 0653Z and 0700Z (fig. 15), a subglacial valley near 40 km wide and extending down to 520 m above sea level in revealed, a valley which can be correlated with outflow areas along the western margin of the ice sheet (Walker, Pearce, and Zanella, 1968). Farther east, from 0700Z to 0805Z, there is a relatively uniform 0.2 percent slope to the east, down which the ice increases in thickness to a maximum value of 2,450 m. Between 0805Z and 0908Z, the bottom of the glacier is generally beneath sea level, extending to a maximum depth of 300 m below sea level. The thickest ice measured on the eastbound leg, about 2,700 m, is found in this region.

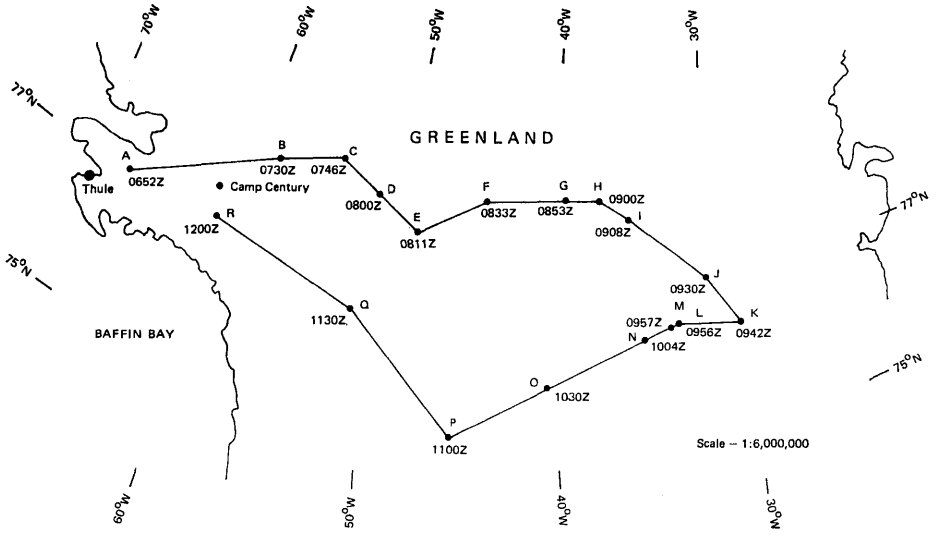

FIGURE 15. Map showing the course of Flight 1 (from Walker, Pearce, and Zanella, 1968).

Between stations 0908Z and 0942Z, ice-surface elevations are nearly constant at 2,400 m above sea level, and ice thickness decreases to the east. The subglacial terrain becomes increasingly mountainous as the eastern highlands are approached (near 0942Z). These subglacial hills are also revealed at the beginning of the westward leg of the traverse, from 0942Z to nearly 1015Z (fig. 17).

From 1015Z to 1042Z, farther west along the westward leg of the traverse, the bottom again dips beneath sea level. However, less of the subglacial terrain along this leg of the traverse is beneath sea level than along the more northerly eastbound route. In addition, the maximum depth of the bottom is only about 200 m below sea level, compared with the minimum of 300 m below sea level observed in the eastward flight. The maximum ice thickness measured in Flight 1, about 2,900 m, occurs in this area.

A broad subglacial hill, about 300 m high and about 50 km wide, is present near station 1003Z. From this point westward, the elevation of the bottom fluctuates between 0 and 200 m above sea level, with the ice thinning toward the west to nearly 1,400 m.

Numerous irregularities in the upper surface of the ice are shown in the profiles (figs. 16 and 17), particularly on the westward leg of Flight 1 (fig. 17). These irregularities, in many places mirrored by similar irregularities in the bottom, are principally due, in the author's opinion, to errors in the determination of the ice-surface elevation rather than to actual changes in the profile. It is impossible to

separate this error from genuine abrupt ice-surface elevation changes, so they are shown in figs. 16 and 17; however, the author believes that the surface of the ice sheet is, in fact, smoother than is shown in the profiles, and that these irregularities probably do not exist.

SUMMARY

Airborne radar sounding has been used successfully to collect data permitting the calculation of the thickness of a portion of the Greenland ice sheet. The empirical technique developed in this paper relates the dielectric properties of ice with its thickness, and is used for the reduction of the data collected during several flights over the ice sheet.

Airborne ice-thickness soundings are a rapid, mobile, and accurate method to survey the thickness of ice sheets and glaciers. At present, the most serious limitation is the navigational error, although recent advances in the development of precise navigational systems should overcome this obstacle.

In the area surveyed, ice thicknesses were generally 2,000 m, though maximums of 2,900 m and minimums of 100 m were recorded. In general, thinner ice occurred over subice hills and thicker ice was present where the subice surface was lower, particularly where it occurred at elevations below sea level.

REFERENCES

Bailey, J. T., S. Evans, and **G. de Q. Robin.** 1964. Radio echo sounding of polar ice sheets. Nature 204: 1309–1314.

Evans, S. 1963. Dielectric properties of ice and show—A review. J. Glaciology 5: 773–792.

Gow, A. J., H. T. Ueda, and **D. E. Garfield.** 1968. Antarctic ice sheet: Preliminary results of first core hole to bedrock. Sci. 171: 1011–1013.

Jiracek, G. R. 1965. Radio sounding of Antarctica ice. Unpub. M.Sc. Thesis, Univ. of Wisc. 172 p.

Pawlowicz, E. F. 1969. An isostatic study of northern and central Greenland based on gravity values and airborne radar ice-thickness measurements. Tech. Rept. R–619, Naval Civil Engineering Laboratory, Port Hueneme, Calif. 98 p.

Pearce, D. C. and **J. W. Walker.** 1967. An empirical determination of the relative dielectric constant of the Greenland ice cap. J. Geophy. Res. 72: 5743–5747.

Robin, G. de Q. 1967. Internal reflecting layers within ice sheets. Paper presented at International Meeting of Radio Echo Sounding of Ice and Glaciers, Strasbourg, France.

Robin, G. de Q. and **S. Evans.** 1967. Electromagnetic properties of ice and snow. Paper presented at International Meeting of Radio Echo Sounding of Ice and Glaciers, Strasbourg, France.

Swithinbank, C. 1967. Radio echo sounding of Antarctic glaciers from light aircraft. Paper presented at International Meeting of Radio Echo Sounding of Ice and Glaciers, Strasbourg, France.

Von Hippel, A. R. 1954. Dielectrics and waves. John Wiley and Sons, New York. 284 p.

Walker, J. W., D. C. Pearce, and **A. H. Zanella.** 1968. Airborne radar sounding of the Greenland ice cap: flight 1. Bull. Geol. Soc. Amer. 79: 1639–1646.

Weber, J. R. and **P. Andrieux.** 1970. Radar soundings on the Penny ice cap, Baffin Island. J. Glaciology 9: 49–53.